45th AIAA Aerospace Sciences Meeting and Exhibit
8 - 11 January 2007, Reno, Nevada

AIAA 2007-1060

Further Development of a High-Speed Three-Dimensional Flow Visualization System

Brian S. Thurow* and Aman Satija†
Advanced Laser Diagnostics Laboratory
Auburn University, AL 36849

Further development of a high-speed three-dimensional flow visualization system is explored. The technique is based on the high-speed scanning and imaging of a laser sheet produced by a pulse burst laser capable of operating in excess of 1 MHz. The focus of this study is on the characteristics of a galvanometric scanning mirror and its subsequent use within a 3-D imaging system. The maximum angular velocity of the mirror is in excess of 100,000 degrees/second over a 150 microsecond period with the mirror capable of accessing over 18 resolvable spots every 1 µsec. Preliminary three-dimensional images of rising incense smoke were acquired by operating the system in a "low-speed" mode with a 15 mW HeNe laser and a high-speed camera operating at 1,000 fps. In this configuration, each 3-D image (220 x 220 x 68 voxel resolution) took 67 msec to acquire. Sample 3-D images are presented that demonstrate the technique's capability to visualize complex, three-dimensional flow structures, such as those associated with the transition to turbulence in rising smoke. Future work will concentrate on incorporating the pulse burst laser into the imaging system and should increase the speed by 2-3 orders of magnitude making the technique suitable for higher speed flows.

I. Introduction

Techniques available for flow diagnostics have witnessed an evolution from intrusive pitot-tubes to non-intrusive techniques using lasers. In the past, laser based flow diagnostics were limited spatially to one-dimension such as with laser doppler anemometry or to two-dimensional techniques like Schlieren imaging or particle image velocimetry. Due to the inherent spatial and temporal limitations of these techniques, many fluid dynamic problems that are three dimensional in character cannot be completely understood. Flow visualization is a powerful tool in the investigation of various flow phenomena, such as turbulence, and the focus of this work is on the development of a high-speed 3-D flow visualization technique.

A number of efforts have been made over the years to develop 3-D flow measurement systems. These include stereographic,[1] holographic,[2-4] tomographic,[5] and laser sheet scanning[6-15] methods. The approach that has received the most attention and is adopted in this effort is laser scanning flow visualization. In this technique, a laser beam, formed into a sheet using cylindrical lenses, is scanned through the flow field using an optical deflector, such as a rotating mirror. As the laser sheet passes through the flow field, a sequence of images at different planes in the flow field is acquired. A 3-D image can then be reconstructed from the stack of images. A significant advantage to this method is that it can utilize many of the measurement concepts and principles already developed for conventional planar techniques, such as particle image velocimetry (PIV) and planar laser induced fluorescence (PLIF). For the most part, however, the application of 3-D diagnostics has been restricted to low-speed flows ($V < 1$ m/s) due to the limited repetition rate of available lasers, cameras and scanning mirrors.

Past efforts, such as those by Long and Yip[7], Yip et al.[8], Patrie et al.[9], Island et al.[11] and Hult et al.[14] have demonstrated the ability to perform these measurements at very high speeds, but broad application and performance of these techniques have been limited by the specialized equipment necessary for their implementation. Recent advances in high-repetition rate laser and camera technology, however, have made much of this equipment more capable and more readily available. This presents a renewed opportunity to develop 3-D flow diagnostics that have the potential to expand their application to a greater number of laboratories.

* Assistant Professor, AIAA Member, Corresponding author: thurow@auburn.edu
† Graduate Research Assistant, AIAA Student Member

The Advanced Laser Diagnostics Laboratory (ALDL) at Auburn University has recently launched an effort to develop a high-speed laser-scanning 3-D flow visualization technique based on a 3rd generation MHz rate pulse burst laser system, a commercially available high-speed camera and a high-speed scanner. **This paper describes recent progress in our efforts to develop the high-speed 3-D imaging technique, including characterization of a high-speed scanning mirror and preliminary 3-D images obtained using a low-speed configuration.** The long-term goal of the work is to develop a high-speed system capable of acquiring a complete 3-D image in tens of microseconds.

II. Three Dimensional Imaging Concept

The chief components of the high speed imaging technique being developed at the ALDL are the pulse burst laser system, a high speed scanning mirror and an ultra-high speed camera. A schematic and photograph of the experimental set-up used in this work is shown in Figure 1. Due to an unexpected equipment failure, a 15 mW HeNe laser was used in place of the pulse burst laser system limiting the speed of the current experiments to a relatively low-speed setting. The overall concept of the high-speed system, however, remains the same and future work is expected to be two to three orders of magnitude faster. The output from the laser is deflected using a galvanometric scanning mirror and formed into a light sheet using a cylindrical lens. Images are then acquired at each subsequent plane and a 3-D image reconstructed from the image sequence. A brief description of each of the main components is given here.

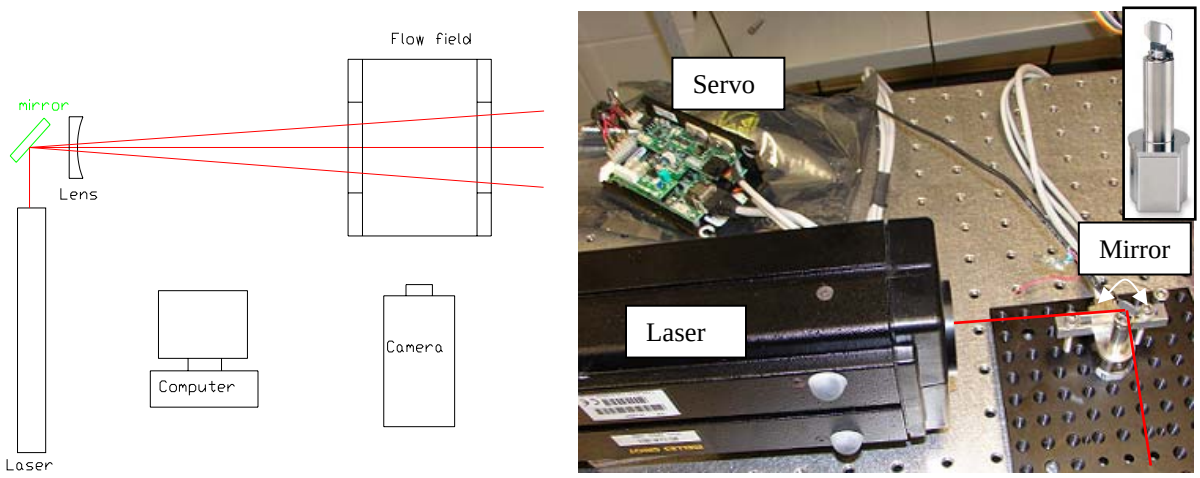

Figure 1: Schematic and photograph of experimental set-up of laser and scanning mirror.

A. Pulse Burst Laser System

Unfortunately, the pulse burst laser system was not available for the present study due to an unexpected failure of one of the electrical components in the system's high voltage power supply. The system has recently been repaired and will be used for future studies. As the pulse burst laser is necessary for achieving the high-speed goals of this project, a brief description of the system is still given here. A more detailed description can be found in Thurow and Satija.[16]

The AU pulse burst laser system is a 3rd generation design based on similar systems described by Lempert et al.[17], Wu et al.[18] and Thurow et al.[19] The basic concept is the formation and amplification of a train of short-duration laser pulses. In the AU system, the pulses are created using a low-power (100 mW) cw Nd:YAG laser and an acousto-optic modulator (AOM), a device traditionally used in some Q-switched lasers. The AOM acts as a high-speed deflector and is used to form the desired pulses by cycling the deflection on and off very rapidly. Each pulse is ~20 nsec in duration and contains ~1 nJ of energy. Repetition rate is only limited by the AOM, which has a bandwidth of 100 MHz. The pulses are then passed through an amplifier chain consisting of three flashlamp pumped, Nd:YAG rod amplifiers. Faraday isolators are used to isolate each amplification stage and avoid parasitic oscillations. The amplifier system has been designed to provide a gain of 10^7 to bring the pulse energy up to ~10 mJ/pulse at 1064 nm. The amplified pulses can then undergo 2nd harmonic generation to 532 nm using a type II

KTP non-linear crystal which has a demonstrated efficiency of 40-50 percent. It should be noted that higher powers are possible through the addition of more amplifiers and 3rd (355 nm) and 4th (266 nm) harmonic generation is also possible.

B. High-speed scanning mirror

In a previous work, we demonstrated the capabilities of an acousto-optic deflector (AOD) to deflect laser pulses at sufficiently high speeds to be used in a 3-D imaging system.[20] The chief advantage of an AOD is that the random access time is as low as 1 µsec, meaning that any random deflection angle can be obtained within 1 µsec. The AOD was marked by two significant shortcomings, however. The first is that the number of resolvable spots that could be obtained under ideal conditions was 50. This greatly limits the ability to use the AOD in higher resolution systems requiring more planes of data. The second, and possibly most important, is that the deflection efficiency ranged from 30 to 60% across all deflection angles. This places an additional demand on the laser and camera system, which must make up for the lost signal.

In this work, we explore the use of a commercially available galvanometric scanning mirror (General Scanning Inc. VM500) to deflect laser pulses. This type of mirror was used in a similar high-speed application by Hult et al.[14] and can achieve sufficiently high speeds over a short period of time. The main drawback to this type of mirror is a relatively long (compared to the AOD) random access time, which limits its use to linear (i.e. one direction) sweeps through the flow field. Characterization of the speed of this mirror is the subject of Section III.

C. High-speed camera

Until recently, the number of ultra-high-speed cameras commercially available was quite scarce and a limiting factor for researchers trying to develop high-speed imaging technique. Fortunately, a large number of ultra-high speed cameras capable of framing rates on the order of 1 MHz are now commercially available. The characteristics of these cameras varies widely. In this work, we use a DRS Hadland Ultra68 for high-speed imaging. This camera combines multiple high-speed imaging methods to obtain 68 images with a resolution of ~240 x 240 pixels at up to 500,000 frames per second. It is also capable of burst framing rate of up to 100,000,000 frames per second in 4 frame bursts.

Light entering the camera is directed along four different paths using a unique four-way beam splitter. Each image is then formed on one quadrant of the surface of a segmented intensifier, with the firing of each quadrant being independently controlled. The intensifier is attached to a masked CCD in which only one out of every 17 pixels is exposed to the light; the remaining pixels serve as on-chip charge storage bins, which allows the camera to be operated at higher frame rates than possible if the image were read out off of the chip. Higher frame rates are achieved by synchronizing the exposure of the CCD with the intensifier resulting in a 68 frame sequence of images.

The beamsplitter, intensifier and CCD mask, which divides the signal and limits the fill factor, add a significant amount of noise to each of the images. The gain of the intensifier, however, is sufficient to overcome this noise with the camera performing quite well in poorly illuminated conditions. For the current application, which is concerned with the imaging of rising smoke using a 15 mW laser, the camera performed quite well. We found the contrast between the smoke and the background sufficient to visualize the unique flow patterns produced by the smoke, but, due to the magnitude of the image noise, would be hesitant to use it with techniques requiring more quantitative information about image intensity.

III. Characterization of a galvanometric scanning mirror

One of the main focuses of the work reported here is to characterize the speed and operation of the scanning mirror, a device with which we had little previous experience. This section discusses these experiments and demonstrates the mirror's ability to work at the high speeds necessary for scanning of the pulse burst laser.

A. Scanning parameters

A scanning system is characterized by the number of resolvable spots it produces, its deflection efficiency, slew rate and random access time. The number of resolvable spots is the number of distinct angular positions that can be attained is given as the ratio of the total scan angle to the divergence of the laser beam:

$$N = \frac{\Delta\alpha}{\Delta\phi} \tag{1}$$

where $\Delta\phi$ is the angular spread of the incident beam and $\Delta\alpha$ is the total deflection angle of the device. The angular spread of a Gaussian laser beam is given as:

$$\Delta\phi = 1.27\frac{\lambda}{D} \qquad (2)$$

where λ is the wavelength and D is the beam's diameter. From Eq. 2 it is observed that a larger aperture would be suitable to produce a larger number of resolvable spots; however, a larger aperture leads to a larger moment of inertia of the mirror constraining the ability of the mirror to move rapidly.

The slew rate denotes the number of resolvable spots accessed per unit time and is thus a measure of the angular velocity of the scanning system. The random access time is the time taken for the deflector to go from one random position to another. A distinction is made between random access time and slew rate, which can give quite different pictures depending on the scan device. For acousto-optic and electro-optic deflectors, the angular deflection is a function of driving frequency and not subjected to mechanical constraints; thus, the slew rate and random access time tend to give similar pictures. The random access time for a scanning mirror, however, is relatively large (100s of µsec) due to the time required to completely start and stop the motion of the mirror. The slew rate, on the other hand, can be quite fast if the mirror is allowed to remain in motion throughout the scan. In addition, the galvanometric mirror has a deflection efficiency of greater than 98%, high damage threshold (>100 MW/cm2) and economical cost making it ideal for the current application.

B. Experiments

Figure 1 contains a photograph of the mirror (GSI Lumonics VM500) along with the 15 mW HeNe laser used in these measurements. A servo (GSI Lumonics MiniSAX) is used to control the mirror with power provided at +/- 15 V using a variable DC power supply (Tenma 72-7245). A positive (+) and negative (-) terminal, with respect to ground, is essential for proper operation of the device. The mirror was controlled by a +/- 3V command input generated using LabView software and a National Instruments data acquisition board (Model 6251). An optical encoder built into the mirror provides feedback of the mirror's position. The mirror is AR coated for 532 nm with reflectivity of over 98%. The maximum scan angle for the mirror is +/- 20 degrees. Figure 2 shows the plot of scan angle vs command input (volts). This figure indicates the linear relationship between the command input and the scan angle.

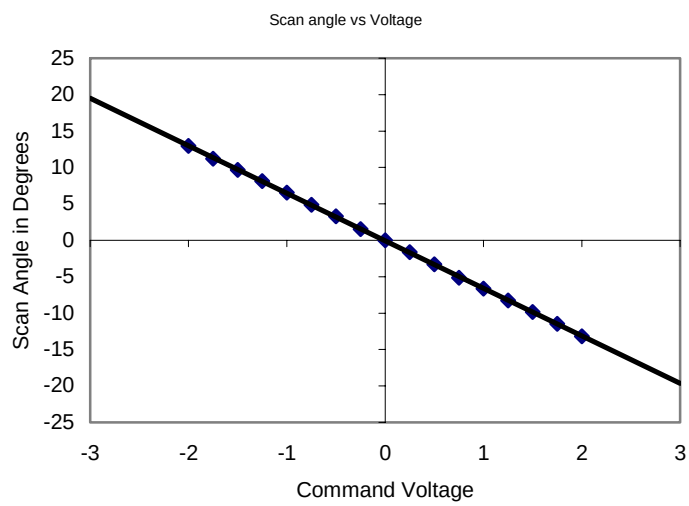

Figure 2: Scan angle vs command input voltage

An important consideration in high speed scanning is the time taken for the mirror to move from one position to the next (i.e. random access time) as well as its angular velocity (i.e. slew rate). Figure 3 shows the response of the mirror to a step command telling it to move its position from -13º to +13 º. The waveform shown in the figure, including the notch that occurs at a time of 1,000 microseconds, was confirmed by imaging the position of a moving laser spot with the high-speed camera. As can be seen, the mirror takes over 1 msec to settle into its

final position, indicating a random access time of over 1 msec. The overshoot is less severe for smaller step angles where the settling time is less than 1 msec.

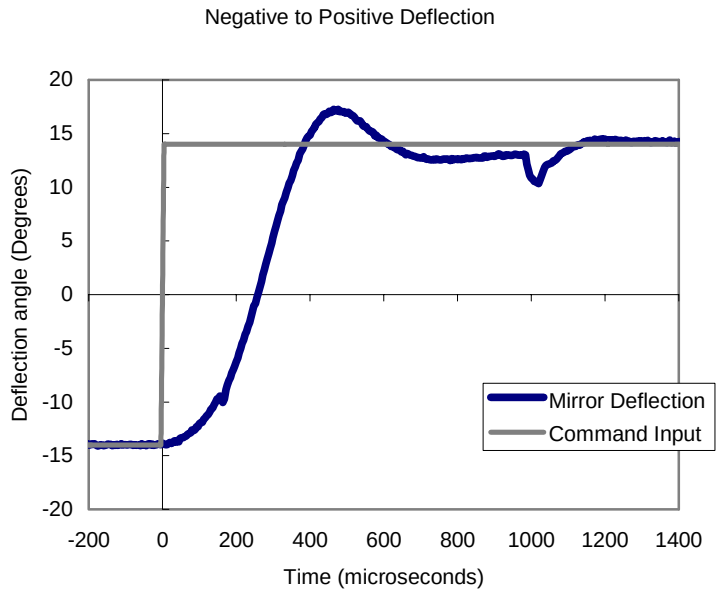

Figure 3: Response (deflection angle) of mirror to a step input command.

For high-speed 3-D imaging, where the mirror does not have to stop at each position, the slew rate is the more relevant parameter to consider. In this case, laser pulses will be deflected while the mirror remains in motion. As the laser pulses are short (~20 nsec), the position of the mirror for that image is effectively constant. The instantaneous speed of the mirror can be estimated by calculating the slope of the curve in Figure 3. This was done using a polynomial curve fit, which made calculation of the derivative somewhat easier. This is shown in Figures 4a (curve fit) and 4b (slope).

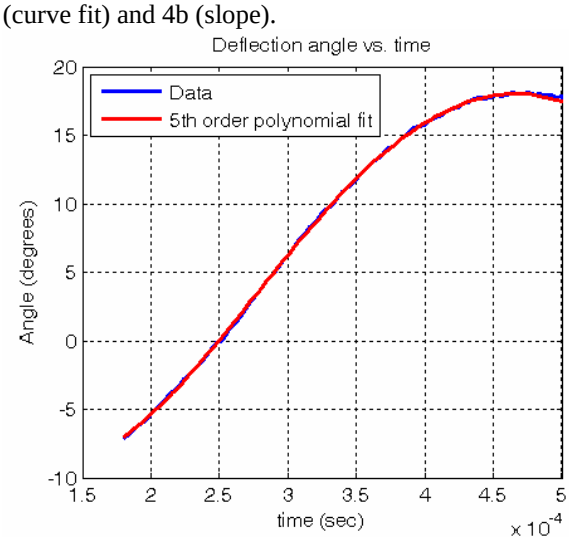

Figure 4a: Polynomial curve fit to data shown in Fig. 3.

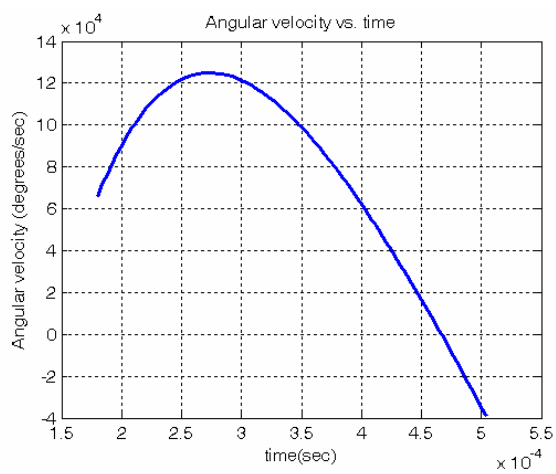

Figure 4b: Angular velocity vs. time for a step input command

Fig. 4b shows that the angular velocity of the mirror exceeds 100,000 deg/sec over a time period lasting ~150 µsec with a maximum speed of ~125,000 deg/sec. Over this time span, the mirror moves approximately 17 degrees. For a 6 mm diameter Gaussian beam at 532 nm, this range corresponds to ~ 2700 resolvable spots with an average slew rate of ~ 18 spots per microsecond. This is an important observation as it clearly shows that the speed

of the mirror is sufficient for very high-speed imaging applications where we would like to acquire multiple planes of data in a few microseconds. In this case, the speed of the mirror is sufficiently fast to acquire 18 planes of data per microsecond. The speed of the mirror can be controlled by modifying the waveform of the command input to a ramp instead of a step or using a smaller step. A large step is necessary in order to allow the mirror to accelerate to high speeds and was chosen in this case to produce the fastest motion of the mirror.

The repeatability of the waveform shown in Figure 3 was determined by imaging a moving spot produced by the laser beam with the high-speed camera. For a fixed time delay after the step input was given, any movement of the spot from its expected position in the image could not be observed, indicating that the motion of the mirror is very repeatable from one command input to the next. Overall, the mirror proves to be a fast, inexpensive, reliable and an efficient scanning system for volumetric imaging.

IV. Three-dimensional Flow Visualization

In order to gain confidence and experience with the mirror and imaging system, a simple set of low-speed 3-D experiments were conducted. This was also necessitated by the temporary unavailability of the pulse burst laser. In the low-speed configuration, light from a 15 mW He-Ne laser was substituted for the pulse burst laser. The high-speed camera, capable of 500,000 fps was operated at 1,000 fps with exposure time of 1 msec for each frame. A staircase waveform generated using LabView was used as command input for the mirror so that the mirror would pause at each deflection angle. The staircase constituted of 68 steps corresponding to 68 image frames, each step being 1 millisecond long. In a high-speed set-up with the pulse burst laser system, the command input will be a single step or ramp and the laser will fire as the mirror moves through the center of sweep.

Rising smoke produced from the burning of four incense sticks was chosen as a simple and convenient method for producing an interesting flow field to demonstrate the capabilities of the technique. Mie scattering from the relatively large smoke particles produced sufficient signal to be detected by the camera even with the relatively low power laser. We estimate that the pulse burst laser (5 mJ/pulse), based on total energy per exposure, would produce roughly 300 times the signal as produced in the present case. The experimental setup is shown in Figure 5. The arrow indicates the direction of laser from the mirror to the incense. Not shown is an enclosure placed around the incense sticks used to mitigate ambient air currents.

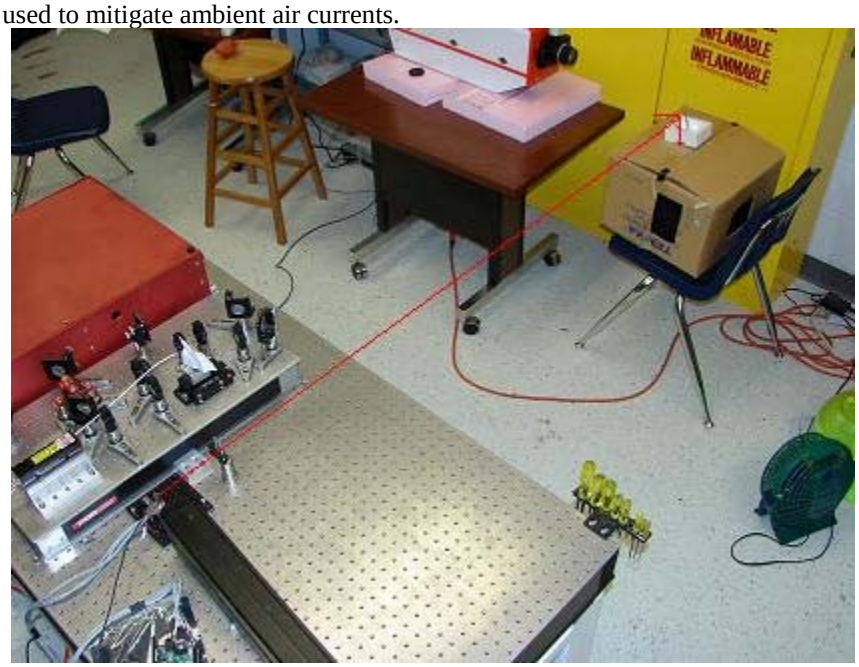

Figure 5: Photograph showing the incense sticks, DRS Hadland camera and the direction of laser propagation.

Figure 6 shows a sequence of 12 images (out of 68) of the laser sheet passing through the incense smoke. Each image in the figure corresponds to a ~3.8” x 3.8” field of view with the sheet thickness being approximately 0.05”. The imaging region was a few inches above the end of the incense sticks where the undisturbed flow

remained laminar throughout the imaging region. It should be noted that each frame corresponds to a different planar slice in the flow field and that any observed motion is due to the 3-D structure of the flow. Matlab was used for image processing, which included a dot card correction and a low-pass filtering of the images to remove some of the random noise introduced by the intensifier and CCD array.

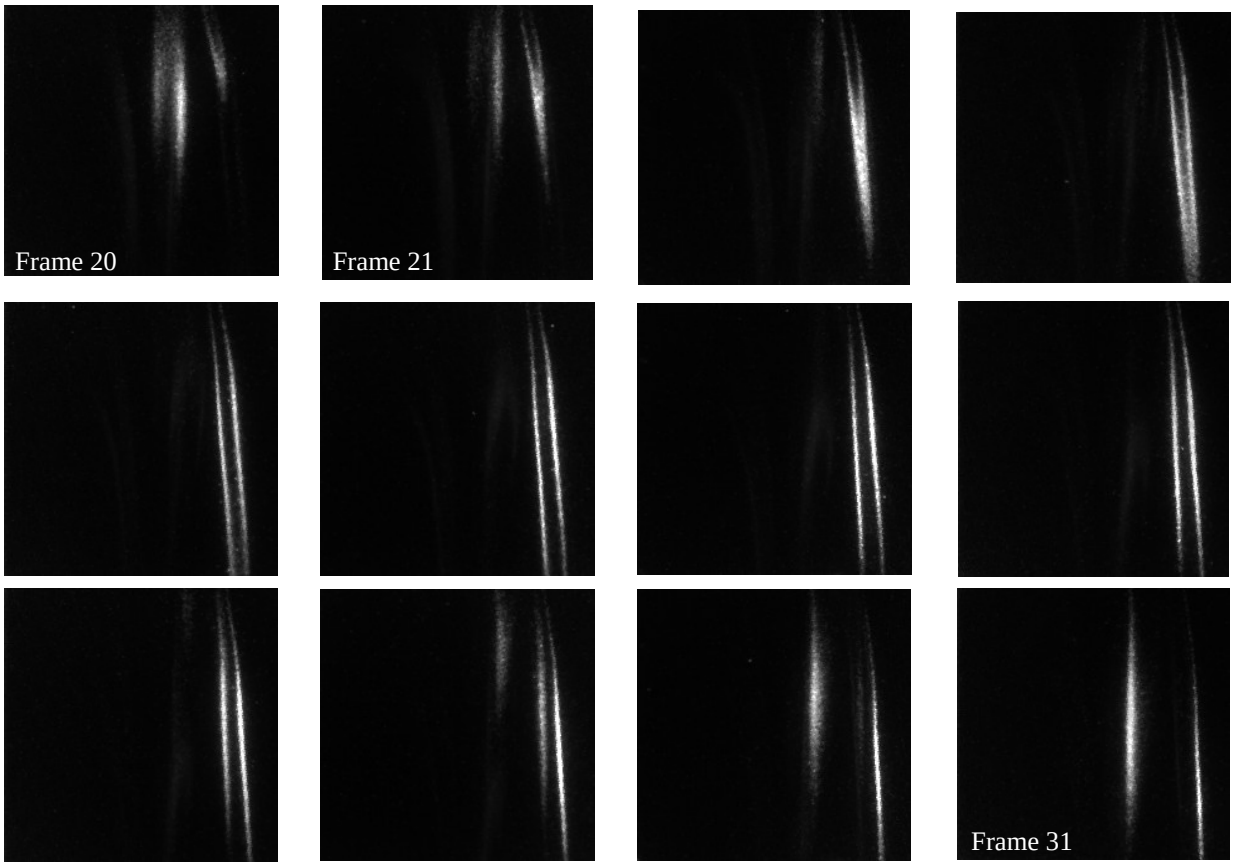

Figure 6: Twelve frames (out of a 68 frame sequence) of the scattering of light from rising smoke. Each frame constitutes a different 2-D slice through the flow field.

The true strength of the imaging technique is, of course, the ability to produce 3-D images. Figure 7a and 7b shows two different views of a reconstructed 3-D image made from the same sequence of images used to produce Figure 6. The images were reconstructed in Matlab using, among others, the function **isosurface.** This function takes three-dimensional scalar data and computes a surface corresponding to a constant value within the 3-D data field. In this case, the value was image intensity with a numerical value of 25 (out of 255) chosen to produce the images in Figure 7. This threshold was above the background noise threshold of the images, but low enough to capture most of the observable flow structure. The contrast between the smoke and the surrounding air was distinct enough that the choice of intensity threshold does not greatly affect the 3-D images presented here. The total volume of the imaging region is 3.8” x 3.8” x 3.1” with an overall 3-D exposure time of 67 msec. We point out that the overall exposure time would be reduced to 134 µsec with the pulse burst laser and the DRS Hadland camera operating at 500,000 fps and can be improved even further using other high speed cameras capable of greater framing rates.

The amount of information contained in Figure 7 is substantial and clearly easier to interpret than the sequence shown in Figure 6. In this case, the flow appears to be laminar and the number of smoke plumes (4) is clear. Even in this laminar case, there are interesting features that would be difficult to identify without use of a 3-D imaging technique. For example, the crescent cross-sectional shape of the smoke plume at the back of the image (upper most plume in 7b) would be difficult to visualize and might be assumed to be round in cross-section based on lesser information. We attribute this particular feature to the smoke rising up and around the incense stick.

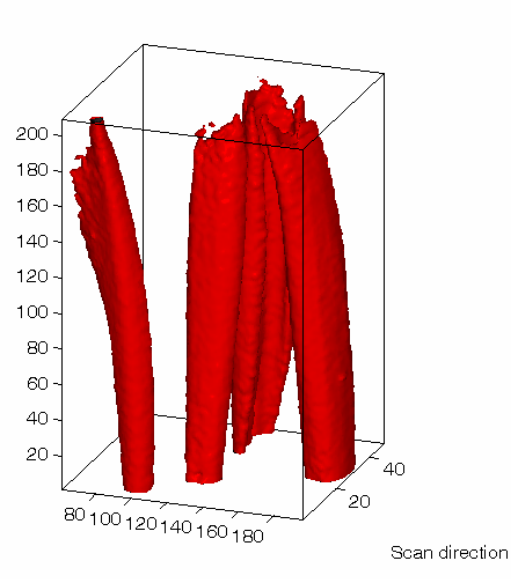

Figure 7a: 3-D picture of smoke rising from four incense sticks. Image is taken within the laminar regime of the flow.

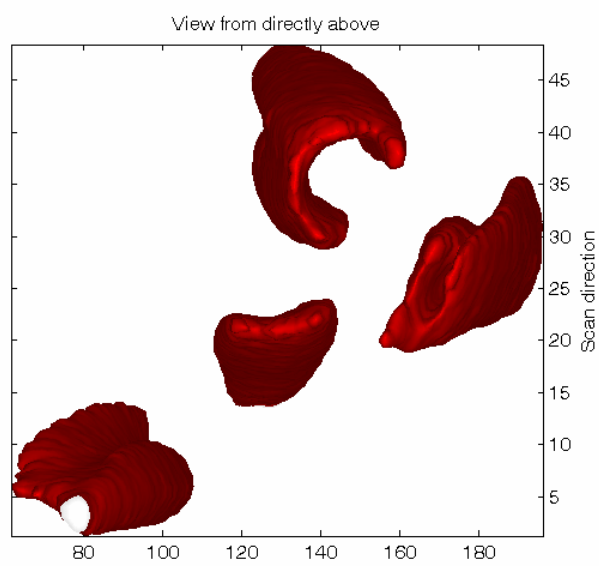

Figure 7b: Overhead view of Fig. 7a showing more detail about the 3-D structure of the smoke plumes.

The tremendous potential of the technique for 3-D flow visualization becomes even clearer when the flow is disturbed by shaking the base holding the incense sticks. This causes the flow to transition from the laminar to the turbulent flow regime and leads to interaction between the four smoke plumes. This is marked by the formation of highly three-dimensional vortical structures. One such case is shown in Figures 8a and 8b where the flow is clearly three-dimensional. Of note is a large-scale vortical structure near the front of the image. Figure 8b shows a close-up cross-sectional view of the structure and depicts some of the interior details of the 3-D image. Viewed in 2-D, the structure appears as a mushroom vortex without any indication of the 3-D structure seen in Figure 8a. Other apparent details include the waviness of the rising smoke plume and the various interactions throughout the measurement volume.

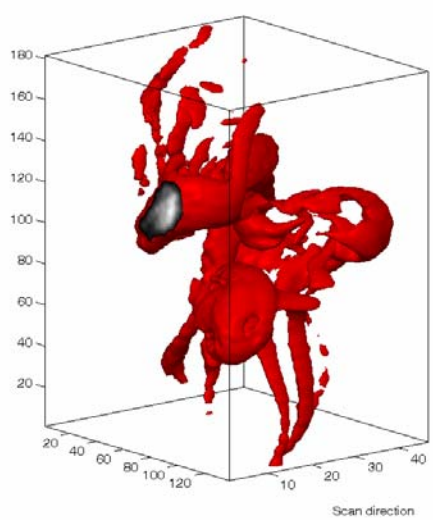

Figure 8a: 3-D image of smoke subjected to a disturbance forcing transition.

Figure 8b: Close-up and cut-away view of vertical structure near the forefront for Fig. 8a.

Figures 9 and 10 show two more 3-D flow images produced using this technique. The image in Fig. 9 appears to show some of the features associated with the transition from laminar to turbulent flow as indicated by

the smooth intertwining interaction of the plumes. Figure 10, on the other hand, seems to depict a flow that has progressed further through the transition process as the individual plumes become less distinct and the structures more irregular. The reader is encouraged to take a close look at these figures to appreciate the wealth of information they contain.

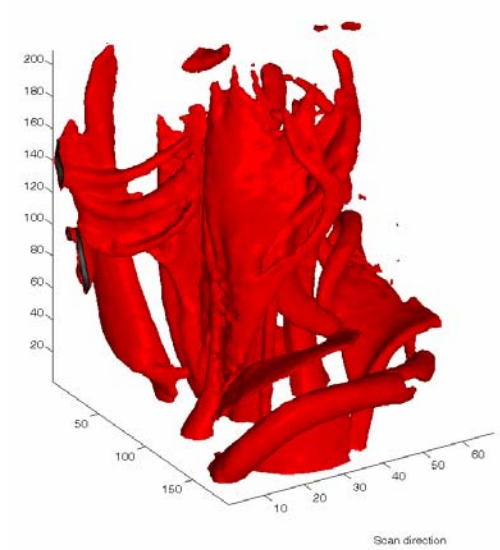

Figure 9: 3-D image of interacting smoke plumes as they transition to turbulent flow.

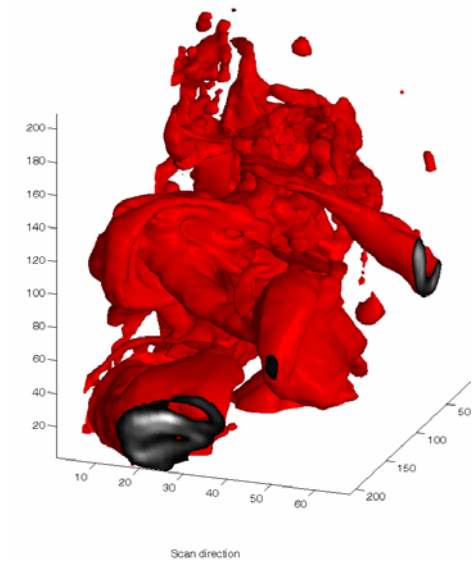

Figure 10: 3-D image of interacting smoke plumes.

V. Conclusions and Future Work

Decent progress towards developing a high-speed 3-D flow visualization technique has been made. The main focus of this work was on the high-speed characteristics of a galvanometric scanning mirror and its implementation into a low-speed 3-D imaging system. The long-term focus, however, remains on the high-speed aspects of the system. One conclusion from the present work is that the galvanometric mirror, which is capable of producing greater than 10^7 resolvable spots per second over a short period of time, is sufficiently fast for the desired scanning of the pulse burst laser beam. The main limiting factor, therefore, appears to be the speed of the ultra-high-speed camera. The camera used in this work is limited to 500,000 fps over 68 frames, but this can be improved upon using other commercially available cameras. The next step in the development of the technique is to incorporate the pulse burst laser into the 3-D imaging system and verify the ability to synchronize the mirror's motion with the firing of the laser and the camera. In addition, we plan on investigating other aspects unique to 3-D imaging, such as the depth of field produced by the lens system and the change in magnification over the measurement volume.

Even without the pulse burst laser system being available for the current set of experiments, the 3-D images produced here are quite interesting and demonstrate the potential of 3-D imaging techniques to reveal features about the flow that could not be observed otherwise. This was observed in the complex 3-D vortical structures produced within a smoke plume from a simple incense stick. These experiments also helped lay the ground work and build up experience for moving on to a higher speed technique. Much more is now understood about the control of the mirror as well as the processing and displaying of 3-D images. In this case, very simple 3-D visualization tools were used and we look forward to applying 3-D visualization techniques available in commercial software packages such as TecPlot.

It is also interesting to note that what we call "low-speed" may, in fact, be fast enough for many other applications. All that was needed for the current experiments was a HeNe laser, a scanning mirror and a high-speed camera. The laser and camera are components that may be readily available in other laboratories and the scanning mirror can be acquired relatively inexpensively (~$2k). Thus, the present results illustrate that many laboratories may have the capacity to perform 3-D flow visualization with already existing equipment. One potentially interesting application would be to couple the current technique with a high-speed CMOS camera (e.g. Vision Research, Photron, or Red Lake), which is capable of sustaining frame rates of 1,000 fps over several thousand images. This would enable time-resolved 3-D flow-visualization where 3-D flow visualization movies could be produced.

VI. Acknowledgments

The support of the Army Research Office (program manager: Dr. Thomas Doligalski) through the Young Investigator Program is gratefully acknowledged. The authors wish to thank Brad Diedrick for his help in setting up and developing the mirror's control system and Zhiguo Xu for his help in designing and conducting the experiments.

VII. References

1 Guezennec, Y.G., Brodkey, R.S., Trigui, J. and Kent, J.C. "Algorithms for fully automated three-dimensional particle tracking velocimetry," Exp. in Fluids, Vol. 17, pp. 209-219, 1994.

2 Royer, H., "Holography and particle image velocimetry," Meas. Sci. Technol., Vol. 8, pp. 1562-1572, 1997.

3 Trolinger, J.D., Rottenkolber, M. and Elandaloussi, F, Meas. Sci. Technol., Vol. 8, pp. 1573-1583, 1997.

4 Sheng, J. Malkiel, E., and Katz, J., "Single beam two-views holographic particle image velocimetry," App. Optics, Vol. 42, pp. 235-250, 2003.

5 Elkins, C.J., Markl, M., Pelc., N. and Eaton, J.K., "4D Magnetic resonance velocimetry for mean velocity measurements in complex turbulent flows," Exp. Fluids, Vol. 34, pp. 494-503, 2003.

6 Kychakoff, G., Paul, P.H., Van Cruyningen, I, and Hanson, R.K., "Movies and 3-D Images of Flowfields Using Planar Laser-Induced Fluorescence," App. Optics, Vol. 26, pp. 2498-2500, 1987.

7 Long, M.B. and Yip, B., "Measurement of Three-Dimensional Concentrations in Turbulent Jets and Flames," Proc. 21st Symp. on Comb., pp. 701-709, 1988.

8 Yip, B., Schmitt, R.L., and Long, M.B., "Instantaneous, Three-Dimensional Concentration Measurements in Turbulent Jets and Flames," Opt. Letters, Vol. 13, pp. 96-98, 1988.

9 Patrie, B.J., Seitzman, J.M., and Hanson, R.K., "Instantaneous Three-Dimensional Flow Visualization by Rapid Acquisition of Multiple Planar Flow Images," Opt. Eng., vol. 33, pp. 975-980, 1994.

10 Goldstein, J.E. and Smits, A. J., "Flow Visualization of the Three-Dimensional, Time-Evolving Structure of a Turbulent Boundary Layer," Phys. Fluids, Vol. 6, pp. 577-587, 1994.

11 Island, T.C., Patrie, B.J., Mungal, M.G. and Hanson, R.K., "Instantaneous Three-Dimensional Flow Visualization of a Supersonic Mixing Layer," Exp. Fluids, Vol. 20, pp. 249-256, 1996.

12 Brucker, CH, "3D scanning PIV applied to an air flow in a motored engine using digital high-speed video," Meas. Sci. Technol., Vol. 8, pp. 1480-1492, 1997.

13 Delo, C and Smits, A.J., "Volumetric Visualization of Coherent Structure in a Low Reynolds Number Turbulent Boundary Layer," Int. J. of Fluid Dyn., Vol. 1, 1997.

14 Hult, J., Omrane, A., Nygren, J., Kaminski, C.F., Axelsson, B., Collin, R., Bengtsson, P.-E., and Alden, M., "Quantitative Three-Dimensional Imaging of Soot Volume Fraction in Turbulent Non-Premixed Flames," Exp. Fluids, Vol. 33, pp. 265-69, 2002.

15 Tian, X. and Roberts, P.J.W., "A 3D LIF System For Turbulent Buoyant Jet Flows," Exp. Fluids, Vol. 35, pp. 636-647, 2003. efficiency of 40-50 percent. Other harmonics are also available.

16 Thurow, B. and Satija, A., "Characteristics of a 10 MHz Repetition Rate Pulse Burst Laser System at Auburn University," AIAA Paper 2006-1384, 44th AIAA Aerospace Sciences Meeting and Exhibit, Reno, NV, 2006.

17 Lempert, W. R., Wu., P., Zhang, B., Miles, R. B., Lowrance, J. L., Mastracola, V., and Kosonocky, W. F., "Pulse-burst laser system for high speed flow diagnostics," AIAA Paper 96-0179, (1996).

18 Wu, P., Lempert, W. R., and Miles, R. B., "MHz pulse-burst laser system and visualization of shock-wave/boundary-layer interaction in a Mach 2.5 wind tunnel," AIAA J., Vol. 38, 672, (2000).

19 Thurow, B., Jiang, N., Lempert, W. and Samimy, M., "A MHz Rate Pulse Burst Laser for High-Speed Flow Diagnostics," Applied Optics, Vol. 43, No. 26, pp. 5064-5073, September 2004.

20 Thurow, B. and Satija, A., "Preliminary Development of a Nearly-Instantaneous Three- Dimensional Imaging Technique for High-Speed Flow Fields," AIAA Paper 2006-2972, 25th Aerodynamic Measurement Technology and Ground Testing Conference, San Francisco, CA, June 2006.